CHEMISTRY
A EUROPEAN JOURNAL

DOI: 10.1002/chem.200701009

A Borogermanate with Three-Dimensional Open-Framework Layers

Ding-Bang Xiong,[a, b] Jing-Tai Zhao,*[a] Hao-Hong Chen,[a] and Xin-Xin Yang[a]

Abstract: A layered borogermanate with three-dimensional microporosity within the layers, $K_4[B_8Ge_2O_{17}(OH)_2]$ (monoclinic, space group: $C2/c$; $a=12.095(2)$, $b=6.7979(14)$, $c=19.944(4)$ Å; $\beta=93.04(3)°$; $V=1637.6(6)$ Å^3; $Z=4$), has been synthesized in a flux of potassium borate. Because of its three-dimensional pore structure and thermal stability, the compound has the potential to eventually form nanocomposites with polymers and to be processed into thin microporous films.

Keywords: borogermanates · building blocks · flux synthesis · layered compounds · microporous materials

Introduction

Layered materials are often considered as a subset of porous materials.[1] Depending on the structure of the layers, they fall into three classes, namely materials with dense nonporous layers, with microporous sheet layers, and with three-dimensional microporous layers.[2] Compounds belonging to the third class are of particular interest because they open up the possibility of a route towards combined microporous–mesoporous materials. However, although materials with porous sheet layers of the second group are relatively common,[3–5] to the best of our knowledge, there have been only two examples of materials with three-dimensional microporous layers. One is an aluminosilicate (ITQ-2), which has large pores running within the layer and smaller six-membered ring (6MR)[1] transport-limiting openings perpendicular to the layer.[6] The first truly three-dimensional microporous layered material is a strontium silicate (AMH-3), reported by Tsapatsis and co-workers,[2,7] with 8MR apertures both perpendicular to and within the silicate layers. Herein, we report the synthesis and structure of a layered potassium borogermanate, $K_4[B_8Ge_2O_{17}(OH)_2]$, with similar three-dimensional open-framework layers. We studied this system because: 1) compared to the silicates, the germanates have smaller Ge-O-Ge angles and b) germanium and boron are more diverse in their coordinations with oxygen and have generated many new borogermanates with porous structures.[8–17]

Initially, we noticed that the structures of $K_2[Ge(B_4O_9)]\cdot 2H_2O$,[13] reported by Yang et al. and the compound used for its synthesis, $K_2[B_4O_5(OH)_4]\cdot 2H_2O$,[18] contain a similar borate unit made of two nearly perpendicular rings of polyhedra, $[B_4O_9H_x]$. The unit in the latter, $[B_4O_5(OH)_4]^{2-}$, is fully protonated and isolated, while that in the former is completely deprotonated and condensed with four GeO_4 groups at the formerly protonated oxygen atoms to form a three-dimensional (3D) open framework (Figure 1). We were interested in eventual intermediates in which deprotonation of one, two, or three hydroxyl groups followed by condensation may lead to chain or layer compounds. Low-temperature synthesis in fluxes has proven to work well for these systems[8,18] and this approach was used for the synthesis of $K_4[B_8Ge_2O_{17}(OH)_2]$.

Results and Discussion

Colorless crystals of the new compound were obtained as a single-phase product (>98% yield based on GeO_2) by heating a mixture of $K_2[B_4O_5(OH)]\cdot 2H_2O$ and GeO_2 in a molar ratio of 2:1 at 280 °C for seven days, whereby the former served as both flux and reagent. A platelike crystal of suitable size was selected for single-crystal X-ray diffraction analysis (Table 1). Electron probe X-ray microanalyzer (EPMA)

[a] Dr. D.-B. Xiong, Prof. Dr. J.-T. Zhao, Dr. H.-H. Chen, X.-X. Yang
The State Key Laboratory of High Performance Ceramics and Superfine Microstructure, Shanghai Institute of Ceramics
Chinese Academy of Science
Shanghai 200050 (PR China)
Fax: (+86) 21-5241-3122
E-mail: jtzhao@mail.sic.ac.cn

[b] Dr. D.-B. Xiong
Graduate School of Chinese Academy of Science Beijing
19 Yuquan Road, Beijing 100049 (PR China)

Supporting information for this article is available on the WWW under http://www.chemistry.org or from the author.

[1] Throughout the manuscript 6MR etc. refers to the number of tetrahedron centers in the ring system.

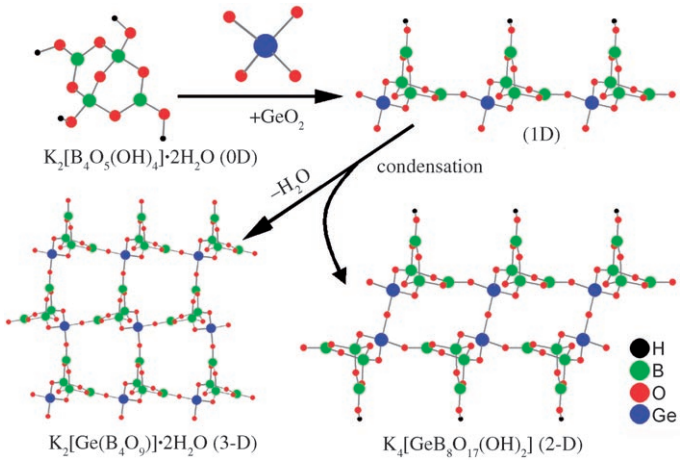

Figure 1. The isolated and fully protonated units $[B_4O_5(OH)_4]^{2-}$ in $K_2[B_4O_5(OH)_4]\cdot 2H_2O$ (upper left) can condense into a 3D framework after complete deprotonation as in $K_2[Ge(B_4O_9)]\cdot 2H_2O$ (lower left). Partial deprotonation may lead to chain (upper right) and layer (lower right) structures.

Table 1. Crystallographic data and refinement parameters for $K_4[B_8Ge_2O_{17}(OH)_2]$.

Empirical formula	$K_4[B_8Ge_2O_{17}(OH)_2]$
F_w	694.08
radiation, λ [Å]	$Mo_{K\alpha}$, 0.71073
crystal system	monoclinic
space group	*C*2/*c* (no. 15)
unit cell dimensions	
a [Å]	12.095(2)
b [Å]	6.7979(14)
c [Å]	19.944(4)
β [°]	93.04(3)
V [Å^3]	1637.6(6)
Z	4
crystal size [mm^3]	$0.05\times0.05\times0.04$
ρ_{calcd} [g cm^{-3}]	2.815
$\mu(Mo_{K\alpha})$ [mm^{-1}]	4.795
θ range for data collection [°]	2.05 to 27.16
R_{int}/R_σ	0.0332/0.0454
no. of refined parameters	155
measured data	3968
unique data	1807
data [$I>2\sigma(I)$]	1576
GooF	0.989
final *R* indices [$I>2\sigma(I)$]	
R_1[a]	0.0295
wR_2[b]	0.0645
R indices (all data)	
R_1	0.0357
wR_2	0.0663
largest diff. peak and hole [e Å^{-3}]	−0.582, 0.589

[a] $R_1=\Sigma||F_o|-|F_c||/\Sigma|F_o|$. [b] $wR_2=\{\Sigma[w(F_o^2-F_c^2)^2]/\Sigma[w(F_o^2)^2]\}^{1/2}$.

data gave a ratio of 1.9:1 for K:Ge. TG-DTA-MS analysis carried out in a flow of Ar showed a weight loss of 4.5% in three steps between 30 and 630 °C. The first step before 200 °C is attributed to the gradual loss of adsorbed water (1%), and the last two steps (3.5%) are assigned to the loss of hydroxyl groups (calcd 2.59%) and the removal of the volatile boron oxide phase. The material is thermally stable up to 440 °C, but becomes amorphous after heating at 650 °C for 0.5 h.

The layers in $K_4[B_8Ge_2O_{17}(OH)_2]$ (Figure 2) are thick and each comprise two interconnected porous sheets, A and B. Both sheets have a honeycomb (3.9) topology, but are mutually rotated by 180°. They contain GeO_4 tetrahedra bonded to three partially deprotonated $B_4O_8(OH)$ units. The two sheets are linked via the fourth oxygen atoms of the GeO_4 tetrahedra, which, in turn, form Ge_2O_7 dimers. The terminal hydroxyl groups of $B_4O_8(OH)$ point outward from the layers and are involved in hydrogen bonding between them (O–H···O distances between 2.814 and 3.052 Å). Selected bond lengths and angles for this compound are presented in Table 2. The potassium cations reside both between the layers as well as between the AB sheets within the layers.

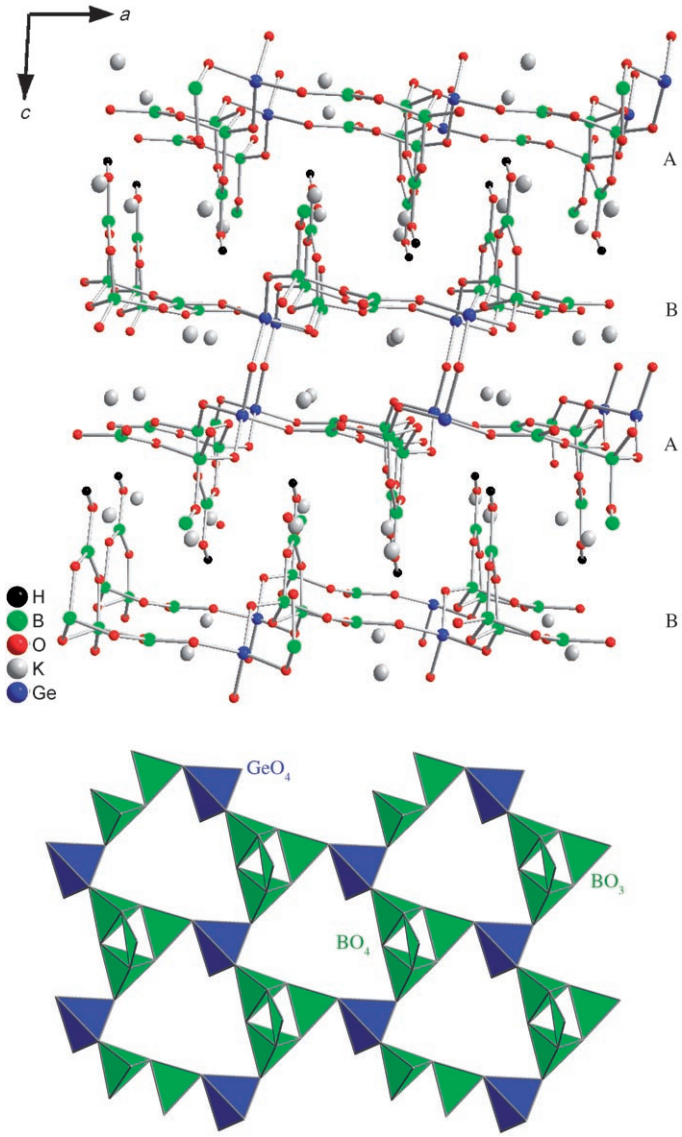

Figure 2. Top: A view of $K_4[B_8Ge_2O_{17}(OH)_2]$ along the layers and its eight-membered ring channels parallel to the *b* axis. Bottom: The connectivity between borate and germanate groups in the single A or B borogermanate sheets.

Table 2. Selected bond lengths [Å] and angles [°] in $K_4[B_8Ge_2O_{17}(OH)_2]$.[a]

Ge–O7	1.724(2)	O7-Ge-O2	120.71(11)
Ge–O2	1.728(2)	O7-Ge-O3	106.28(11)
Ge–O3	1.755(14)	O2-Ge-O3	107.60(9)
Ge–O4	1.762(2)	O7-Ge-O4	105.23(10)
		O2-Ge-O4	107.08(10)
		O3-Ge-O4	109.67(8)
B1–O5	1.350(4)	O5-B1-O9	124.5(3)
B1–O9	1.352(4)	O5-B1-O4	114.8(3)
B1–O4	1.399(4)	O9-B1-O4	120.7(3)
B2–O5	1.484(4)	O1-B2-O7	115.0(3)
B2–O10	1.516(4)	O1-B2-O5	109.7(3)
B2–O7	1.462(4)	O7-B2-O5	109.9(3)
B2–O1	1.444(4)	O1-B2-O10	110.3(3)
		O7-B2-O10	103.3(2)
		O5-B2-O10	108.3(3)
B3–O1	1.450(4)	O1-B3-O2	113.6(3)
B3–O2	1.457(4)	O1-B3-O8	110.2(3)
B3–O8	1.491(4)	O2-B3-O8	109.2(3)
B3–O9	1.504(4)	O1-B3-O9	110.0(3)
		O2-B3-O9	107.0(3)
		O8-B3-O9	106.6(3)
B4–O10	1.349(4)	O10-B4-O8	123.8(3)
B4–O8	1.368(4)	O10-B4-O6	122.8(3)
B4–O6	1.376(4)	O8-B4-O6	113.3(3)

[a] Bond valence sums (Σs): $[GeO_4]$ tetrahedron, Σs[Ge–O] = 4.07; $[B1O_3]$ trigonal, Σs[B1–O] = 3.04; $[B2O_4]$ tetrahedron, Σs[B2–O] = 3.02; $[B3O_4]$ tetrahedron, Σs[B3–O] = 3.02; $[B4O_3]$ trigonal, Σs[B4–O] = 3.06.

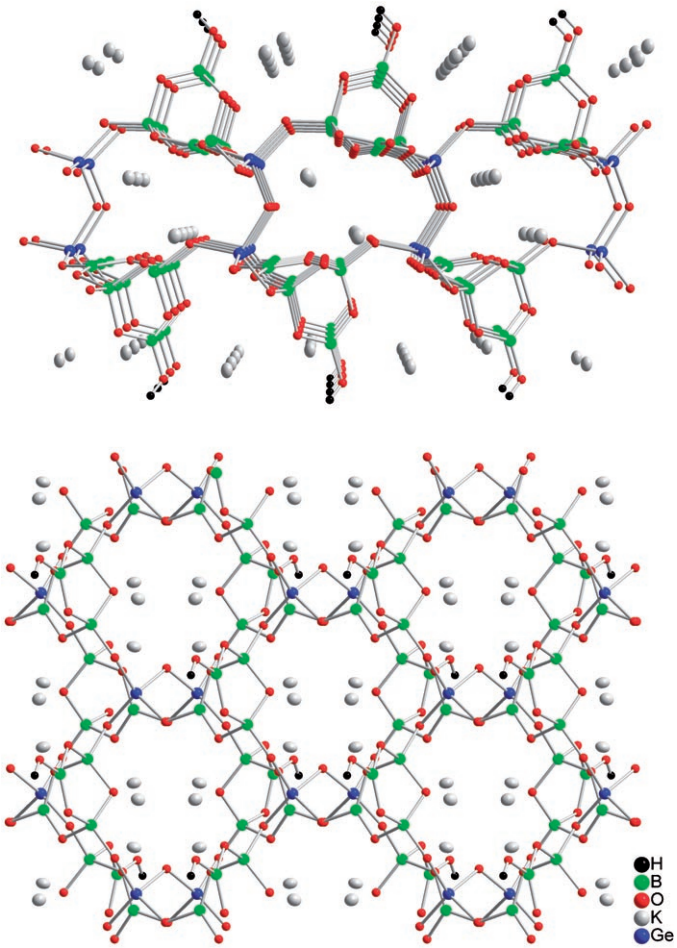

Figure 3. Projections of a single layer along [110] (top) and [101] (bottom) showing 8MR and 9MR channels, respectively.

This specific connectivity between the $B_4O_8(OH)$ and Ge_2O_7 groups gives rise to the three-dimensional porosity of the layers. Thus, each layer has intersecting channels along three directions: 8MR channels along [010] (Figure 2, top) and [110] (Figure 3, top), and 9MR channels along [101] (Figure 3, bottom). Both the [010] and [110] apertures possess interweaving right- and left-handed helical channels. The 9MR channels along [101] are formed from three GeO_4 tetrahedra and three pairs of BO_3 triangles and BO_4 tetrahedra with the following sequence: -(GeO_4)-(BO_4)-(BO_3)-(GeO_4)-(BO_4)-(BO_3)-(GeO_4)-(BO_4)-(BO_4).

Comparison of the structure of $K_4[B_8Ge_2O_{17}(OH)_2]$ with that of AMH-3 reveals some differences. Firstly, within the layer, both $K_4[B_8Ge_2O_{17}(OH)_2]$ and AMH-3 have two 8MR channels parallel to the layer, but AMH-3 has an additional 10MR channel along the [011] direction. Secondly, the transport paths perpendicular to the layers are different. For $K_4[B_8Ge_2O_{17}(OH)_2]$, both the transport path in a single layer and the one created by two sheets from adjacent layers are 9MR channels with the same axis, whereas the axes of the two sets of 8MR channels in AMH-3 are mutually offset. Finally, AMH-3 is built of pure silicon, whereas $K_4[B_8Ge_2O_{17}(OH)_2]$ contains two kinds of cluster units with different compositions, which is important for adjusting the acid strength of zeolite-based catalysts. Although the cluster unit is normal in borogermanates, to the best of our knowledge, there has hitherto been only one example containing more than one type of cluster.[10,12] It is anticipated that the pore size and shape in borogermanate three-dimensional microporous layers may be further adjusted by introducing different Ge–O clusters, within reasonable limits, as molecular building units.[22–24]

Both layered $K_4[B_8Ge_2O_{17}(OH)_2]$ and 3D $K_2[Ge(B_4O_9)]\cdot 2H_2O$ were prepared by using $K_2[B_4O_5(OH)]\cdot 2H_2O$ as a boron source, but different synthetic conditions resulted in different products. $K_2[Ge(B_4O_9)]\cdot 2H_2O$ was synthesized in a mixture of water and organic solvent, in which nucleation and growth are so fast that the detection of the borogermanate precursors is difficult, whereas in a low-temperature synthesis in flux, the kinetics of the hydrolysis and condensation reactions is sufficiently decreased such that intermediates $K_4[B_8Ge_2O_{17}(OH)_2]$ are obtained. Successful synthesis of $K_4[B_8Ge_2O_{17}(OH)_2]$ is of fundamental interest in understanding the relationship between 0D isolated building units, 1D chain, 2D layered, and 3D framework structures, and also sheds some light on the construction of similar layered structures in other systems, such as aluminophosphates and aluminosilicates.

Conclusions

The new layered borogermanate, $K_4[B_8Ge_2O_{17}(OH)_2]$, with three-dimensional open-framework layers, may open the way to the synthesis of similar and other layered microporous solids. Its structure exhibits a unique linkage mode of two types of cluster units, $B_4O_8(OH)$ and Ge_2O_7, that form channels along three different directions. The layered nature of the material suggests that exfoliation of the layers may be possible. This, in turn, may lead to the preparation of polymer–borogermanate nanocomposites[25,26] or precursors of thin microporous films.[27]

Experimental Section

Crystals of $K_4[B_8Ge_2O_{17}(OH)_2]$ were prepared from a flux of $K_2B_4O_5(OH)_4{\cdot}2H_2O$ in a Teflon-lined stainless steel autoclave ($V=$ 20 mL). The autoclave was charged with a mixture of $K_2B_4O_5(OH)_4{\cdot}2H_2O$ (3.06 g, 10 mmol) and GeO_2 (hexagonal phase) (0.53 g, 5 mmol). The reaction was carried out at 280 °C for six days. The autoclave was allowed to cool to room temperature in the furnace. The excess $K_2B_4O_5(OH)_4{\cdot}2H_2O$ was removed by thoroughly washing the product with warm (50 °C) distilled water, and the product was finally dried at 60 °C in air (>98 % yield based on GeO_2) for further characterization. Crystals used for single-crystal structure determination were obtained in a similar fashion. The X-ray powder diffraction pattern was consistent with that calculated from the structure determined by single-crystal X-ray diffraction analysis. To investigate the thermal stability of this compound, samples were heated at different temperatures for 0.5 h, and then cooled to room temperature for further X-ray diffraction analysis.

The crystal shape and elemental composition were studied by means of an electron probe X-ray microanalyzer (EPMA) and an accessory energy-dispersive spectrometer (EDS) on a JXA-8100 microscope. Thermogravimetric analyses (TGA) and differential scanning calorimetry (DSC) combined with mass spectrometry (MS) were performed on a NETZSCH STA-449 C/Balzers MID apparatus at a heating rate of 10 K min^{-1} in a flow of Ar over the temperature range 20–700 °C. IR spectra were collected on a Digilab FTS-80 spectrophotometer by using samples pressed in KBr pellets.

Crystal structure determination: Nonius Kappa CCD diffractometer ($Mo_{K\alpha}$ radiation, $\lambda=0.71073$ Å) at room temperature. The data were corrected for absorption by using the SADABS program.[20] The structure was solved by direct methods and refined against $|F^2|$ with the aid of the SHELXTL-97 software package.[21] After anisotropic refinement of the heavier atoms, the hydrogen atoms were located from the difference Fourier maps and refined without applying any restraints. Further details of the crystal structure investigation can be obtained from the Fachinformationszentrum Karlsruhe, 76344 Eggenstein-Leopoldshafen (Germany; fax: (+49) 7247-808-666; e-mail: crysdata@fiz-karlsruhe.de) on quoting the depository number CSD-417983.

Acknowledgements

This work was supported by the Key Project (no. 50332050) from the NNSF of China, the Hundred Talents Program from the Chinese Academy of Sciences, and the Fund for Young Leading Researchers from the Shanghai municipal government. We are also grateful for the great support from the Max Planck Institute of Chemical Physics of Solids at Dresden, our CAS-MPG partner group. Helpful discussions with Prof. S.C. Sevov of the University of Notre Dame are also greatly acknowledged.

[1] A. Corma, *Chem. Rev.* **1997**, *97*, 2373.
[2] H. K. Jeong, S. Nair, T. Vogt, L. C. Dickinson, M. Tsapatsis, *Nat. Mater.* **2003**, *2*, 53.
[3] M. E. Leonowicz, S. L. Lawton, M. K. Rubin, *Science* **1994**, *264*, 1910.
[4] B. Wei, J. H. Yu, Z. Shi, S. L. Qiu, J. Y. Li, *J. Chem. Soc. Dalton Trans.* **2000**, 1979.
[5] A. Corma, U. Diaz, M. E. Domine, V. Fornes, *J. Am. Chem. Soc.* **2000**, *122*, 2804.
[6] A. Corma, V. Fornes, S. B. Pergher, T. L. Maesen, J. G. Buglass, *Nature* **1998**, *396*, 353.
[7] S. Nair, Z. Chowdhuri, I. Peral, D. A. Neumann, L. C. Dickinson, G. Tompsett, H. K. Jeong, M. Tsapatsis, *Phys. Rev. B* **2005**, *71*, 104301.
[8] M. O'Keeffe, O. M. Yaghi, *Chem. Eur. J.* **1999**, *5*, 2796 and references therein.
[9] D. B. Xiong, H. H. Chen, M. R. Li, X. X. Yang, J. T. Zhao, *Inorg. Chem.* **2006**, *45*, 9301.
[10] Y. F. Li, X. D. Zou, *Angew. Chem.* **2005**, *117*, 2048; *Angew. Chem. Int. Ed.* **2005**, *44*, 2012.
[11] G. M. Wang, Y. Q. Sun, G. Y. Yang, *Cryst. Growth Des.* **2005**, *5*, 313.
[12] H. X. Zhang, J. Zhang, S. T. Zheng, G. Y. Yang, *Inorg. Chem.* **2005**, *44*, 1166.
[13] H. X. Zhang, J. Zhang, S. T. Zheng, G. M. Wang, G. Y. Yang, *Inorg. Chem.* **2004**, *43*, 6148.
[14] Z. E. Lin, J. Zhang, G. Y. Yang, *Inorg. Chem.* **2003**, *42*, 1797.
[15] Y. F. Li, X. D. Zou, *Acta Crystallogr. Sect. C* **2003**, *59*, m471.
[16] M. S. Dadachov, K. Sun, T. Conradsson, X. D. Zou, *Angew. Chem.* **2000**, *112*, 3820; *Angew. Chem. Int. Ed.* **2000**, *39*, 3674.
[17] G. Heymann, H. Huppertz, *J. Solid State Chem.* **2006**, *179*, 370.
[18] M. Marezio, H. A. Plettinger, W. H. Zachariasen, *Acta Crystallogr.* **1963**, *16*, 975.
[19] L. Y. Li, X. L. Jin, G. B. Li, Y. X. Wang, F. H. Liao, G. Q. Yao, J. H. Lin, *Chem. Mater.* **2003**, *15*, 2253.
[20] a) R. H. Blessing, *Acta Crystallogr. Sect. A* **1995**, *51*, 33; b) SADABS: Area-Detector Absorption Correction, Bruker AXS, Madison, WI, **1996**.
[21] G. M. Sheldrick, SHELXTL Programs, release version 5.1; Bruker AXS, Madison, WI, **1998**.
[22] M. O'Keeffe, M. Eddaoudi, H. Li, T. Reineke, O. M. Yaghi, *J. Solid State Chem.* **2000**, *152*, 3.
[23] G. Ferey, *J. Solid State Chem.* **2000**, *152*, 37.
[24] G. Ferey, C. Mellot-Draznieks, T. Loiseu, *Solid State Sci.* **2003**, *5*, 79.
[25] R. Krishnamoorti, R. A. Vaia, E. P. Giannelis, *Chem. Mater.* **1996**, *8*, 1728.
[26] Z. Wang, T. J. Pinnavaia, *Chem. Mater.* **1998**, *10*, 1820.
[27] Y. Umemura, A. Yamagishi, R. Schoonheydt, A. Persoons, F. De Schryver, *Langmuir* **2001**, *17*, 449.

Received: July 3, 2007
Published online: October 15, 2007

